

IR Simulation Model Validation Notes

Findings Term-Structure Diagnostics

Amine Badii

December 19, 2025

Contents

1 Scope and objective	2
2 Finding 1 — Absence of Pathwise Arbitrage-Free Term-Structure Dynamics	2
2.1 Finding statement	2
2.2 Model features giving rise to the finding	2
2.3 Risk implications for PFE	2
2.4 Validation strategy and diagnostics	2
2.5 Empirical evidence and plots	3
2.6 Conclusion	7
A Appendix A — Theory background	8
A.1 No-arbitrage relationships used in diagnostics	8
A.2 Pathwise vs marginal consistency	8
A.3 Benchmark rationale: Hull–White one-factor (HW1F)	8
B Appendix B — Formal diagnostic definitions	8
B.1 Static discount-factor monotonicity test	8
B.2 Kink index: cross-tenor smoothness diagnostic	9
B.3 Discount-factor wedge: multiplicative consistency diagnostic	9
B.4 Interpretation and complementarity	9
C Appendix C — Algorithmic implementation and benchmark model	9
C.1 Hull–White one-factor (HW1F) model	9
C.1.1 Zero-coupon bond prices	10
C.1.2 Calibration	10
C.2 Algorithmic computation of diagnostics	10
C.2.1 DF monotonicity heatmap	10
C.2.2 Kink index bands	10
C.2.3 Wedge statistics	10
C.3 Reproducibility and governance considerations	10

1 Scope and objective

This document substantiates key validation findings for the interest-rate simulation framework used for PFE, with emphasis on pathwise arbitrage diagnostics and benchmarking against an arbitrage-free reference model (HW1F).

2 Finding 1 — Absence of Pathwise Arbitrage-Free Term-Structure Dynamics

2.1 Finding statement

The IR simulation model does not enforce arbitrage-free term-structure relationships along individual simulation paths. Zero rates at each maturity pillar are simulated independently, with cross-tenor dependence introduced solely through correlations between latent stochastic drivers. As a result, static and dynamic no-arbitrage identities governing discount factors and forward-rate reconstruction may be violated along individual paths, particularly at long horizons and under elevated volatility conditions.

2.2 Model features giving rise to the finding

The finding arises directly from the structural design of the model:

- Each maturity pillar is driven by a dedicated stochastic process calibrated independently to market-implied variance targets.
- Cross-tenor dependence is introduced via correlations between drivers rather than through a unified term-structure factor model.
- No short-rate representation or arbitrage-free drift restriction (e.g. HJM consistency) is imposed.

While this construction ensures marginal calibration accuracy at each tenor, it does not guarantee global coherence of the simulated yield curve along individual paths.

2.3 Risk implications for PFE

The absence of arbitrage-free dynamics may lead to:

- Violations of static discount-factor monotonicity across maturities.
- Reduced cross-tenor smoothness, resulting in locally implausible curve shapes.
- Inconsistencies in discount-factor reconstruction over time, which may accumulate with maturity and affect long-dated exposure profiles.

These effects are expected to be more pronounced for long-horizon PFE metrics and portfolios with significant sensitivity to the shape of the yield curve.

2.4 Validation strategy and diagnostics

Three complementary diagnostics are implemented:

1. **Static discount-factor monotonicity** across maturities.
2. **Cross-tenor smoothness** using a kink index (local curvature proxy).
3. **Pathwise discount-factor multiplicative consistency** via a wedge metric.

All diagnostics are benchmarked against an arbitrage-free Hull–White one-factor (HW1F) model. Together, these diagnostics provide complementary coverage of static, cross-sectional, and dynamic arbitrage constraints.

2.5 Empirical evidence and plots

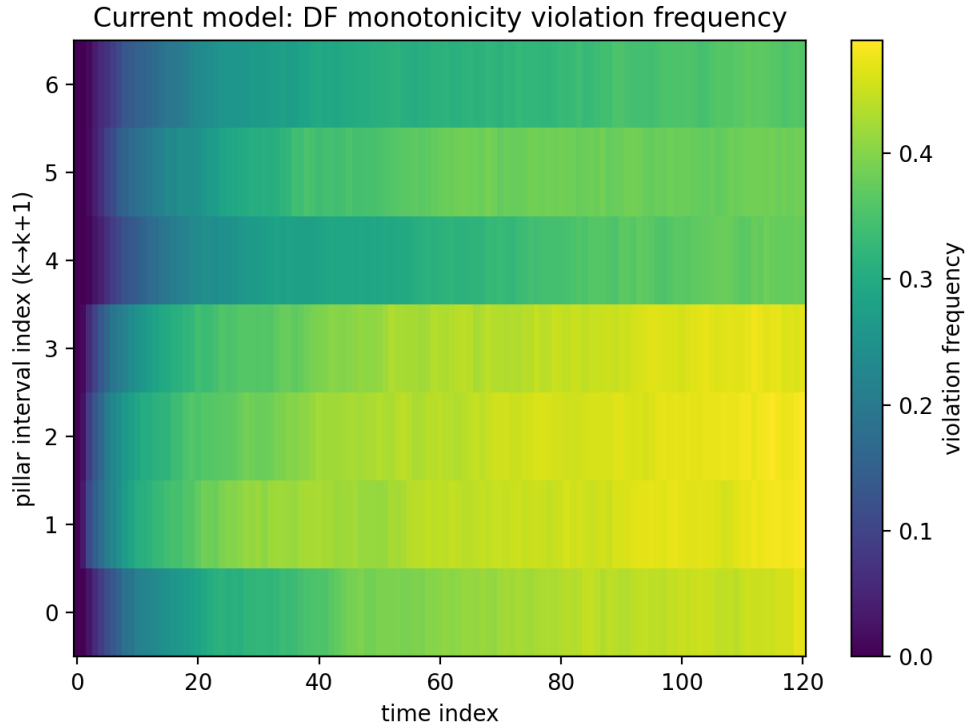


Figure 1: Current model: frequency of discount-factor monotonicity violations across time and pillar intervals.

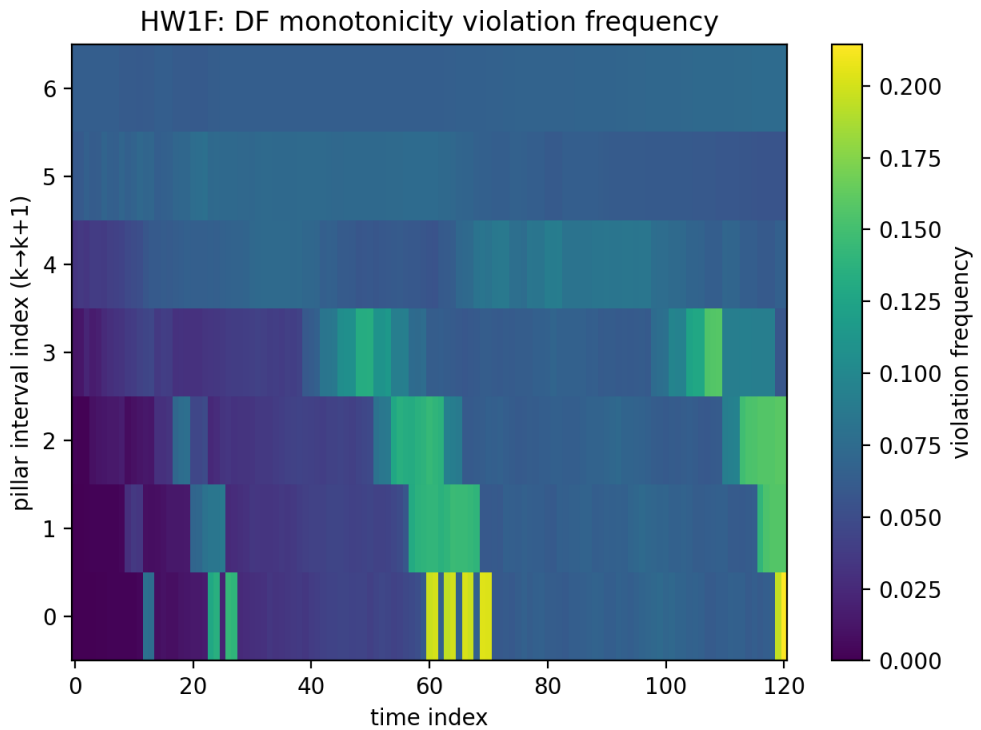


Figure 2: HW1F benchmark: frequency of discount-factor monotonicity violations across time and pillar intervals.

Discount-factor monotonicity violations.

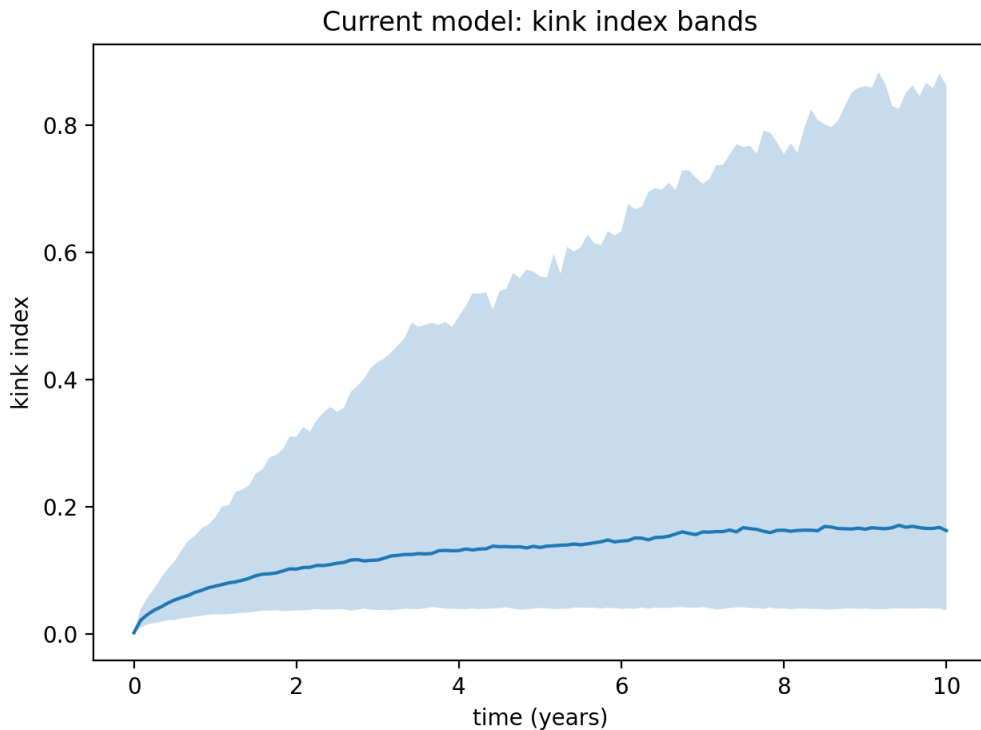


Figure 3: Current model: kink index bands over time (median and dispersion band).

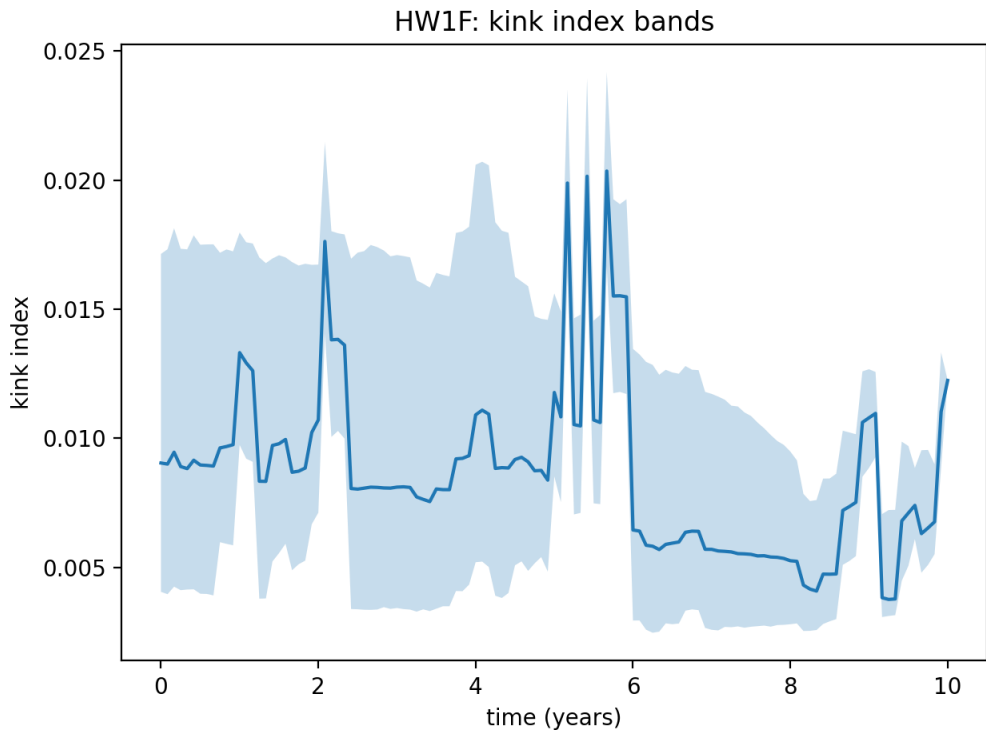


Figure 4: HW1F benchmark: kink index bands over time (median and dispersion band).

Kink index bands (cross-tenor smoothness).

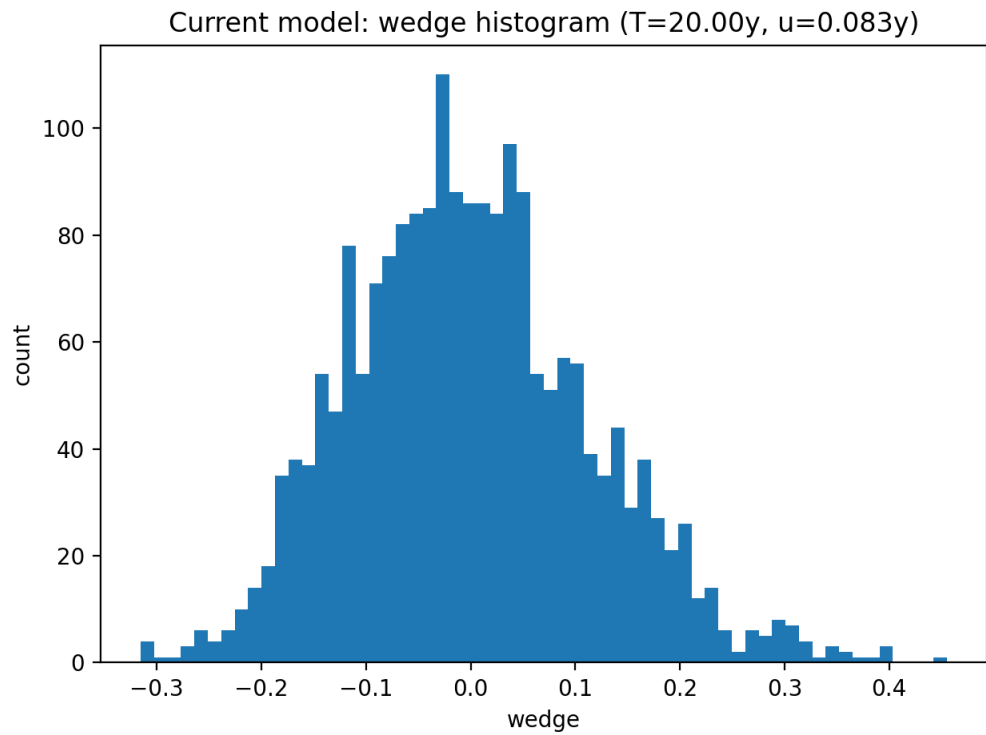


Figure 5: Current model: wedge histogram for a representative (T, u) pair.

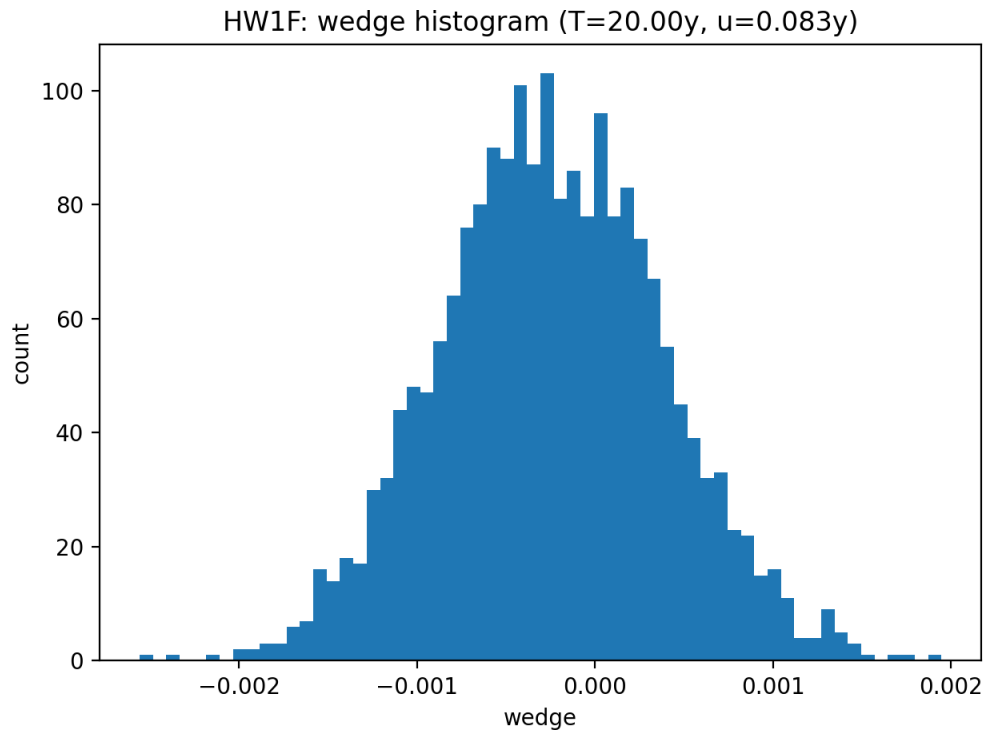


Figure 6: HW1F benchmark: wedge histogram for a representative (T, u) pair.

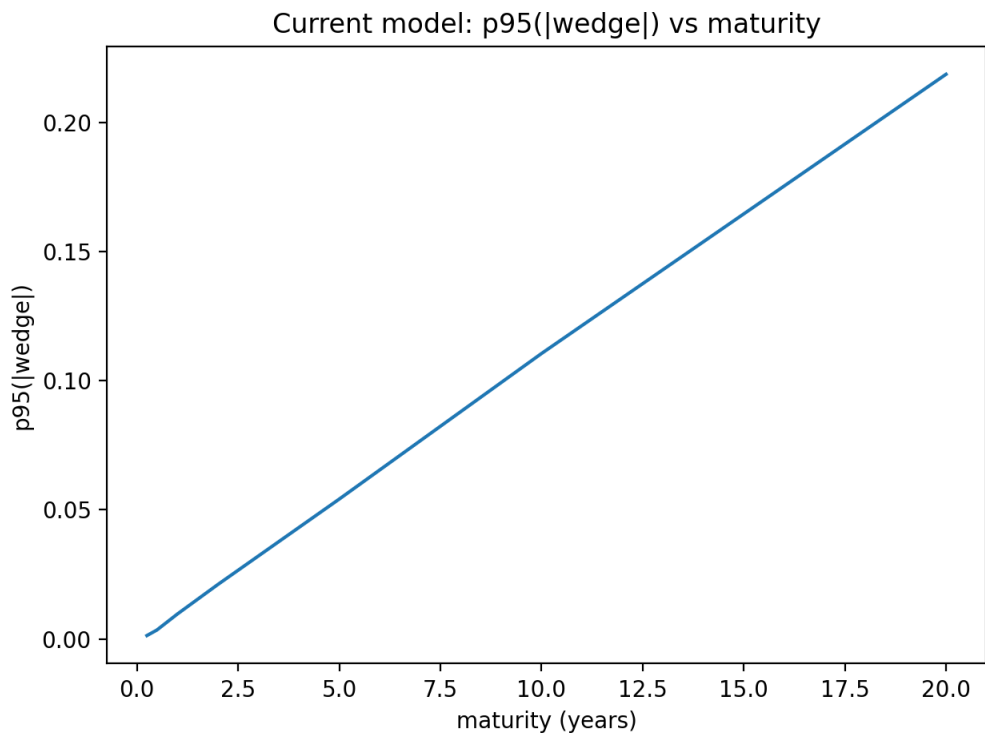


Figure 7: Current model: $p95(|\text{wedge}|)$ vs maturity.

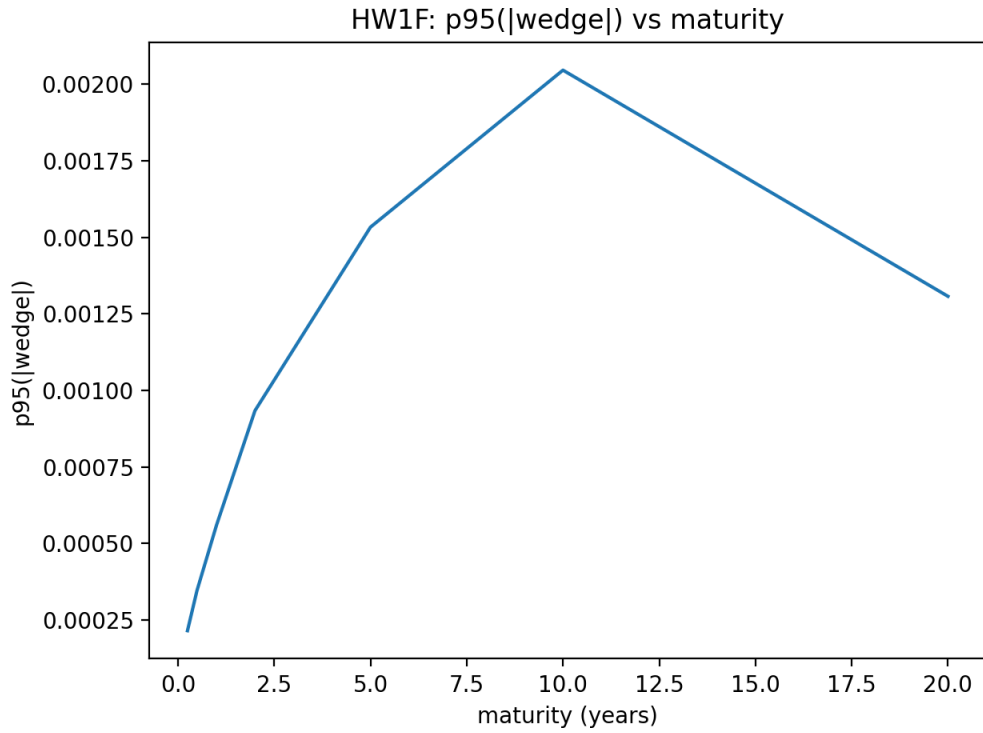


Figure 8: HW1F benchmark: $p95(|\text{wedge}|)$ vs maturity.

Discount-factor wedge (multiplicative consistency).

2.6 Conclusion

The diagnostics demonstrate that the IR simulation model does not enforce pathwise arbitrage-free term-structure dynamics. Violations are systematic and maturity-dependent, and are materially larger than those observed under an arbitrage-free benchmark. This behaviour is a structural consequence of the model design and must be monitored, benchmarked, and appropriately controlled when assessing long-horizon PFE metrics, particularly for long-dated exposure profiles.

A Appendix A — Theory background

A.1 No-arbitrage relationships used in diagnostics

Discount factors and monotonicity. Let $P(t, T)$ denote the discount factor at time t for maturity T . In the absence of negative rates (or under standard admissibility conditions), discount factors are non-increasing in maturity:

$$P(t, T_{k+1}) \leq P(t, T_k) \quad \text{for } T_{k+1} > T_k.$$

Equivalently, using zero rates $z(t, T)$ defined by $P(t, T) = \exp(-z(t, T)(T - t))$, monotonicity may be violated when simulated cross-maturity shapes become inconsistent.

Forward-rate reconstruction identity. For $0 \leq t < T < T + u$, the forward discount factor satisfies

$$P(t, T, T + u) := \frac{P(t, T + u)}{P(t, T)}.$$

Under coherent term-structure dynamics, pricing identities ensure internal consistency of ratios across maturity intervals.

A.2 Pathwise vs marginal consistency

The model may be *marginally consistent* by construction (each maturity pillar calibrated to variance targets), yet not *pathwise consistent* across maturities because:

- the joint evolution across maturities is not derived from a single arbitrage-free term-structure model;
- correlations are imposed at driver level rather than induced by a coherent curve model;
- no drift restriction enforces HJM-consistency.

A.3 Benchmark rationale: Hull–White one-factor (HW1F)

HW1F provides a standard arbitrage-free reference with an explicit short-rate representation. In the benchmark, discount factors and forward ratios inherit consistency properties from the model's term-structure construction (up to numerical error). Therefore, systematic deviations under the current model can be attributed to structural design rather than plotting or discretization.

B Appendix B — Formal diagnostic definitions

B.1 Static discount-factor monotonicity test

Let $\{T_k\}_{k=0}^K$ denote maturity pillars and let $P^{(n)}(t_i, T_k)$ be the simulated discount factor on path n at time t_i .

Define the indicator of a monotonicity violation on path n as:

$$\mathbb{I}_{i,k}^{(n)} = \mathbf{1}\left\{P^{(n)}(t_i, T_{k+1}) > P^{(n)}(t_i, T_k)\right\}.$$

The empirical violation frequency is:

$$\hat{p}_{i,k} = \frac{1}{N} \sum_{n=1}^N \mathbb{I}_{i,k}^{(n)}.$$

This diagnostic captures static violations of the basic no-arbitrage ordering of discount factors across maturities.

B.2 Kink index: cross-tenor smoothness diagnostic

Let $z^{(n)}(t_i, T_k)$ denote the simulated zero rate at pillar T_k . Define the discrete second difference:

$$\Delta^2 z_{i,k}^{(n)} = z^{(n)}(t_i, T_{k+1}) - 2z^{(n)}(t_i, T_k) + z^{(n)}(t_i, T_{k-1}), \quad k = 1, \dots, K-1.$$

The *kink index* for path n at time t_i is defined as:

$$\text{Kink}^{(n)}(t_i) = \sum_{k=1}^{K-1} w_k \left| \Delta^2 z_{i,k}^{(n)} \right|,$$

where w_k are optional scaling weights (e.g. based on maturity spacing).

The kink index measures local curvature and detects abrupt slope changes between adjacent pillars. Large values indicate reduced cross-tenor smoothness and economically implausible curve shapes.

B.3 Discount-factor wedge: multiplicative consistency diagnostic

For a fixed horizon T and increment $u > 0$, define the theoretical identity:

$$P(t, T+u) \equiv P(t, T) P(t, T, T+u).$$

Let $\hat{P}^{(n)}(t; T, T+u)$ denote the forward discount factor reconstructed from simulated quantities (e.g. via zero-rate interpolation).

The *discount-factor wedge* is defined as:

$$\text{Wedge}^{(n)}(t; T, u) = \log P^{(n)}(t, T+u) - \log P^{(n)}(t, T) - \log \hat{P}^{(n)}(t; T, T+u).$$

Under pathwise arbitrage-free dynamics, the wedge should be identically zero (up to numerical error). Persistent dispersion or maturity-dependent growth of the wedge indicates structural inconsistency.

B.4 Interpretation and complementarity

- DF monotonicity tests static arbitrage constraints.
- The kink index captures cross-sectional smoothness and local coherence.
- The wedge diagnostic targets dynamic multiplicative consistency.

Together, these diagnostics provide comprehensive coverage of pathwise arbitrage-free properties.

C Appendix C — Algorithmic implementation and benchmark model

C.1 Hull–White one-factor (HW1F) model

The Hull–White one-factor model specifies the short rate as:

$$r(t) = x(t) + \phi(t),$$

where $x(t)$ follows an Ornstein–Uhlenbeck process:

$$dx(t) = -a x(t) dt + \sigma dW_t.$$

The deterministic shift $\phi(t)$ is chosen to fit the initial term structure exactly.

C.1.1 Zero-coupon bond prices

Under HW1F, the zero-coupon bond price admits the closed form:

$$P(t, T) = A(t, T) \exp(-B(t, T) r(t)),$$

with:

$$B(t, T) = \frac{1 - e^{-a(T-t)}}{a},$$

and $A(t, T)$ determined to match the initial yield curve.

C.1.2 Calibration

Model parameters (a, σ) are calibrated by minimizing the discrepancy between model-implied and market-observed swaption volatilities:

$$\min_{a, \sigma} \sum_i \left(\sigma_{\text{model}}^{\text{swaption}}(i) - \sigma_{\text{market}}^{\text{swaption}}(i) \right)^2.$$

HW1F is arbitrage-free by construction and therefore serves as a suitable benchmark for structural diagnostics.

C.2 Algorithmic computation of diagnostics

C.2.1 DF monotonicity heatmap

For each simulation time and maturity interval:

```
for time i:
    for maturity k:
        violations = mean(DF[:,i,k+1] > DF[:,i,k])
```

C.2.2 Kink index bands

```
for time i:
    for path n:
        kink[n] = sum_k |Z[n,i,k+1] - 2 Z[n,i,k] + Z[n,i,k-1]|
        compute median and quantiles of kink
```

C.2.3 Wedge statistics

```
for maturity T:
    for path n:
        wedge = log(P(T+u)) - log(P(T)) - log(P_hat(T,T+u))
        compute histogram and p95(|wedge|)
```

C.3 Reproducibility and governance considerations

All diagnostics are computed under fixed random seeds and deterministic configuration files. Output artefacts are versioned by model configuration, ensuring traceability between reported figures and underlying simulations.